

## SCALE-FREE EQUILIBRIA OF SELF-GRAVITATING GASEOUS DISKS WITH FLAT ROTATION CURVES

MIR ABBAS JALALI<sup>1</sup>

Institute for Advanced Studies in Basic Sciences, P.O. Box 45195-159, Zanjan, Iran; jalali@iasbs.ac.ir

AND

MEHDI ABOLGHASEMI

Aerospace Research Institute, P.O. Box 15875-3885, Tehran, Iran; mehdi@ari.ac.ir

Received 2002 April 6; accepted 2002 August 1

### ABSTRACT

We introduce exact analytical solutions of the steady state hydrodynamic equations of scale-free, self-gravitating gaseous disks with flat rotation curves. We express the velocity field in terms of a stream function and obtain a third-order ordinary differential equation (ODE) for the angular part of the stream function. We present the closed-form solutions of the obtained ODE and construct hydrodynamical counterparts of the power-law and elliptic disks, for which self-consistent stellar dynamical models are known. We show that the kinematics of the Large Magellanic Cloud can be well explained by our findings for scale-free elliptic disks.

*Subject headings:* galaxies: kinematics and dynamics — galaxies: structure — hydrodynamics — methods: analytical

### 1. INTRODUCTION

Astrophysical disks are either stellar or gaseous. The existence of nonaxisymmetric equilibrium states of such systems has been attractive from both theoretical and observational aspects. The search for dynamical equilibria of stellar systems is known as the self-consistency problem, in which one seeks for a positive phase space distribution function (DF) that produces the density of the model and satisfies the collisionless Boltzmann equation (Binney & Tremaine 1987). The construction of the DF can be done by analytical means or numerical exploration based on Schwarzschild's orbit superposition method (Schwarzschild 1979; Kuijken 1993, hereafter K93; Levine & Sparke 1998; Teuben 1987; de Zeeuw, Hunter, & Schwarzschild 1987; Jalali & de Zeeuw 2002, hereafter JZ02). The main difficulty linked to the self-consistency problem is the lack of the second integral of motion for most planar models.

Gaseous disks, however, are investigated through solving the hydrodynamic equations of compressible, self-gravitating fluids. There are several works in the literature that deal with the stability of perturbed axisymmetric gaseous disks (Heemskerk, Papaloizou, & Savonije 1992; Goodman & Evans 1999; Lemos, Kalnajs, & Lynden-Bell 1991). The problem of nonaxisymmetric systems is somewhat different because our knowledge is limited, even about equilibrium states. Following a first-order linear theory, Syer & Tremaine (1996, hereafter ST96) constructed simple scale-free disks and approximately solved the steady state hydrodynamic equations for the components of the velocity vector. They also proposed a nonlinear theory based on the calculation of Fourier coefficients using Newton's method. A similar strategy was adopted by Galli et al. (2001, hereafter G01) in the study of isothermal molecular clouds and the fragmentation hypothesis of multiple stars. Their nonlinear solutions, in contrast with ST96, were generated by

direct numerical integration of reduced ordinary differential equations (ODEs) and an iterative scheme to match the boundary conditions. These methods of approach seem inefficient when one seeks for global properties of highly nonaxisymmetric equilibria and the transient response of fluid disks in the vicinity of such states. Therefore, finding analytical solutions for the hydrodynamic equations is of special interest, even in steady state conditions.

In this paper we explore exact nonaxisymmetric solutions of self-similar gaseous disks with flat rotation curves. In § 2 we express the governing equations, and we reduce them to a third-order ODE in § 3, in which we also introduce our *closed-form* analytic solutions. We construct hydrodynamical counterparts of the JZ02 models in § 4 and apply our results to the Large Magellanic Cloud (LMC) in § 5. We show that the kinematics of the LMC can be explained by our model elliptic disks. We end up with conclusions in § 6.

### 2. STEADY STATE HYDRODYNAMIC EQUATIONS

We consider a thin disk of compressible, inviscid self-gravitating fluid in a steady state (dynamical equilibrium). The hydrodynamic equations can be written as the time-independent continuity equation,

$$\frac{1}{R} \frac{\partial}{\partial R} (R \Sigma v_R) + \frac{1}{R} \frac{\partial}{\partial \phi} (\Sigma v_\phi) = 0, \quad (1)$$

and the momentum equations,

$$\frac{1}{R} \frac{\partial}{\partial R} (R \Sigma v_R^2) + \frac{1}{R} \frac{\partial}{\partial \phi} (\Sigma v_R v_\phi) - \frac{\Sigma v_\phi^2}{R} = -\frac{\partial p}{\partial R} - \Sigma \frac{\partial U}{\partial R}, \quad (2)$$

$$\begin{aligned} \frac{1}{R} \frac{\partial}{\partial R} (R \Sigma v_R v_\phi) + \frac{1}{R} \frac{\partial}{\partial \phi} (\Sigma v_\phi^2) + \frac{\Sigma v_R v_\phi}{R} \\ = -\frac{1}{R} \frac{\partial p}{\partial \phi} - \Sigma \frac{1}{R} \frac{\partial U}{\partial \phi}, \quad (3) \end{aligned}$$

<sup>1</sup> Scientific Advisor, Aerospace Research Institute, Tehran, Iran.

where  $(R, \phi)$  are the polar coordinates,  $\mathbf{v} = (v_R, v_\phi)$  is the velocity field in the Eulerian description, and  $p$  is the pressure. The potential  $U$  is due to the self-gravity, which is related to the surface density  $\Sigma$  through the Poisson integral,

$$U(R, \phi) = -G \iint \frac{\Sigma(R', \phi') R' dR' d\phi'}{\sqrt{R^2 + R'^2 - 2RR' \cos(\phi - \phi')}} , \quad (4)$$

where  $G$  is the gravitational constant. In § 3 we attempt to simplify the governing equations for scale-free disks and solve the resulting equations by analytical means.

### 3. NONAXISYMMETRIC DISKS WITH LOGARITHMIC POTENTIALS

Gaseous disks with logarithmic potentials possess the astrophysically important property of a flat rotation curve. The circular gaseous disks having this property are known as Mestel (1963) disks, the stabilities of which were investigated by Goodman & Evans (1999). Here we derive *exact analytical* expressions for the physical quantities of non-axisymmetric disks.

#### 3.1. Stream Function

We assume cuspy, scale-free potential-density pairs of the form

$$\begin{aligned} U(R, \phi) &= U_0[2 \ln R + g(\phi)] , \\ \Sigma(R, \phi) &= \frac{\Sigma_0 f(\phi)}{R} , \end{aligned} \quad (5)$$

where  $U_0$  and  $\Sigma_0$  are constants. The functions  $f(\phi)$  and  $g(\phi)$  are  $2\pi$ -periodic in  $\phi$  because they are continuous. We normalize the surface density so that

$$\frac{1}{2\pi} \int_{-\pi}^{\pi} f(\phi) d\phi = 1 . \quad (6)$$

This transfers the scaling of  $\Sigma$  to  $\Sigma_0$  (e.g., G01) and implies  $U_0 = \pi G \Sigma_0$ . Given  $f$ , Poisson's integral does not usually lead to a closed-form expression for  $g$ , and one has to adopt a series solution. Let us assume that  $f(\phi)$  permits the Fourier expansion

$$f(\phi) = 1 + \sum_{l=1}^{\infty} (C_l \cos l\phi + S_l \sin l\phi) , \quad (7)$$

where  $C_l$  and  $S_l$  are constant coefficients. Using equations (A1) and (A5) of ST96, we find the potentials corresponding to single Fourier modes and superpose the results. This gives

$$g(\phi) = -2 \sum_{l=1}^{\infty} \left( \frac{C_l}{l} \cos l\phi + \frac{S_l}{l} \sin l\phi \right) . \quad (8)$$

We prescribe  $f$  and determine  $g$  through the scheme mentioned above. Then, we attempt to solve the momentum equations for  $v_R, v_\phi$ , and the pressure  $p$  in terms of  $f$  and  $g$ .

The velocity components can be derived from the stream function  $\Psi$  as

$$\Sigma v_R = -\frac{1}{R} \frac{\partial \Psi}{\partial \phi} , \quad \Sigma v_\phi = \frac{\partial \Psi}{\partial R} . \quad (9)$$

The scale-free nature of the model suggests the *Ansatz*

$$\Psi(R, \phi) = \Sigma_0 V_\phi [\ln R + P(\phi)] , \quad (10)$$

where  $V_\phi$  is a constant reference velocity that becomes the circular velocity if the disk is axisymmetric ( $f = 1, P = 0$ ). We utilize equations (5)–(10) and take the curl of equations (2) and (3). This eliminates the pressure  $p$  and leaves us with the following ODE for  $P(\phi)$ :

$$P''' - \frac{2f'}{f} P'' + \frac{1}{f^2} [2(f')^2 - ff'' + f^2] P' = \beta f (fg' + 2f') , \quad (11)$$

where  $\beta = U_0/V_\phi^2$  is a dimensionless parameter and the prime denotes  $d/d\phi$ . The solution  $P(\phi)$  results in the velocity field of our planar self-gravitating fluids. Physical solutions of equation (11) correspond to the condition  $\mathbf{v}(R, \phi) = \mathbf{v}(R, \phi + 2\pi)$ , which ensures the continuity of the velocity field. Hence, we seek for  $2\pi$ -periodic solutions of  $P(\phi)$ .

#### 3.2. Velocity Components

Carrying out a change of dependent variable as (this is indeed Liouville's transformation, explained in the Appendix)

$$P' = w(\phi) \frac{f(\phi)}{f(0)} , \quad (12)$$

equation (11) reads

$$w'' + w = \beta f(0) F_0(\phi) , \quad F_0 = fg' + 2f' . \quad (13)$$

The particular solution of equation (13) is then obtained as

$$w(\phi) = \beta f(0) \left[ a_0 \sin \phi + b_0 \cos \phi + \int_0^\phi F_0(s) \sin(\phi - s) ds \right] , \quad (14)$$

where the (dimensionless) constant coefficients  $a_0$  and  $b_0$  are given by

$$\begin{aligned} a_0 &= -\frac{1}{\pi} \int_0^{2\pi} \sin \phi d\phi \int_0^\phi F_0(s) \sin(\phi - s) ds , \\ b_0 &= -\frac{1}{\pi} \int_0^{2\pi} \cos \phi d\phi \int_0^\phi F_0(s) \sin(\phi - s) ds . \end{aligned} \quad (15)$$

The function  $w(\phi)$ , and therefore  $\mathbf{v}$ , is  $2\pi$ -periodic if we impose the boundary conditions  $w(\phi + 2\pi) = w(\phi)$  and  $w'(\phi + 2\pi) = w'(\phi)$ , which lead to the necessary conditions

$$\int_0^{2\pi} F_0(\phi) \sin \phi d\phi = \int_0^{2\pi} F_0(\phi) \cos \phi d\phi = 0 . \quad (16)$$

Using equations (12) and (9), the velocity components are readily determined as

$$\begin{aligned} v_R &= -\beta V_\phi \left[ a_0 \sin \phi + b_0 \cos \phi + \int_0^\phi F_0(s) \sin(\phi - s) ds \right] , \\ v_\phi &= \frac{V_\phi}{f(\phi)} , \end{aligned} \quad (17)$$

from which one can obtain  $P(\phi)$ . It is now straightforward

to determine the pressure  $p$  from either equation (2) or (3) as

$$p = \frac{\Sigma_0 V_\phi^2}{Rf(\phi)} [\beta A(\phi) - 1] = c_s^2 \Sigma, \quad (18)$$

where

$$c_s^2 = \frac{V_\phi^2}{f(\phi)^2} [\beta A(\phi) - 1] \quad (19)$$

is the square of the sound speed (at the azimuth  $\phi$ ) and

$$A(\phi) = f(\phi) \left[ (b_0 \sin \phi - a_0 \cos \phi) + 2f(\phi) - \int_0^\phi F_0(s) \cos(\phi - s) ds \right]. \quad (20)$$

Sound waves are stable if  $c_s^2 > 0$ , i.e.,  $p > 0$ . Define  $A_{\min} = \min\{A(\phi), 0 \leq \phi \leq 2\pi\}$ . The necessary and sufficient condition for the positiveness of  $p$  is

$$0 < \frac{1}{\beta} < A_{\min}. \quad (21)$$

Apart from constraining the admissible values of  $\beta$ , this condition may put some restrictions on the model parameters. As can be seen in equation (17),  $v_\phi$  is maximum where the surface density is minimum, and vice versa. This result has previously been used in the construction of DFs of stellar systems using Schwarzschild's orbit superposition method (e.g., K93; JZ02).

Our scale-free analytical solutions are general. They are independent of special angular variation of surface density and its corresponding potential. Our solutions can be used even in the presence of an external force that falls off as steeply as  $R^{-1}$ . Such a force could be that of a magnetic field or the gravitational influence of a dark matter halo. These effects can enter our equations through  $F_0(\phi)$ .

The most important point related to our solutions is the existence of transonic flows. According to equation (19), it is possible to obtain entirely subsonic, transonic, and entirely supersonic flows depending on the choice of  $\eta = 1/(\beta A_{\min})^{1/2}$  in the range  $0 < \eta < 1$ . Let us define the Mach number

$$M = \frac{1}{c_s} \sqrt{v_R^2 + v_\phi^2}, \quad (22)$$

which is a function of the azimuthal angle  $\phi$  in our disks. For convenience, we use the variable

$$M_0(\phi) = \frac{M - 1}{M + 1} \quad (23)$$

for the classification of flows. Disks with  $M_0(\phi) > 0$  for  $\forall \phi \in [0, 2\pi]$  are entirely supersonic, while for  $M_0(\phi) < 0$  they are subsonic, and our steady state models are credible. Flows for which  $M_0(\phi)$  switches sign along a streamline are transonic. In such a circumstance, steady state models become problematic, as explained below. In principle, transition from subsonic to supersonic speeds (along a streamline) can take place smoothly, but the reverse is impossible without assuming a shock wave, because fluid elements in the subsonic part of a streamline do not have information about the arrival of the particles in the supersonic region of

upstream. Therefore, they suddenly find themselves colliding with these particles. After a while, these interactions develop a shock wave, and the speed of the supersonic stream discontinuously decreases to a subsonic value. This process is inherently time dependent, and it increases entropy and generates heat. Thus, we must cautiously deal with any transonic solution. G01 also argue that models with transonic flows will most likely be unstable. Despite these arguments, there is an exceptional case in nature in which a supersonic flow field is isentropically (and of course smoothly) compressed from supersonic to subsonic speeds. That is the famous ‘‘conical flow,’’ the detailed description of which can be found in Anderson (1990, p. 294). In this very special case, again, a shock wave is still present, but the ‘‘sonic line’’ does not coincide with the shock ray. The latter completely lies in the supersonic region.

In any case, it seems reasonable to exclude transonic solutions from our results. A stability analysis will surely provide much insight into the problem. The instabilities of our nonaxisymmetric disks will be resolved in a future paper.

For axisymmetric disks, the parameter  $\eta$  is obtained in terms of the Mach number through

$$\eta = \frac{M}{\sqrt{1 + M^2}}. \quad (24)$$

In this case,  $M$  is independent of  $\phi$ , and the transition from subsonic to supersonic flows occurs at  $\eta = 1/\sqrt{2}$ .

#### 4. EXAMPLES

We now apply our analytical tool to certain nonaxisymmetric models for which we have either observational evidence or stellar dynamical counterparts.

##### 4.1. Simple Disks

The simplest form of a nonaxisymmetric disk is obtained when a circular disk is perturbed by a single Fourier mode as

$$f(\phi) = 1 + f_m \cos m\phi, \quad (25)$$

where  $0 \leq |f_m| < 1$ . The corresponding  $\phi$ -dependence of the potential becomes

$$g(\phi) = -\frac{2}{m} f_m \cos m\phi. \quad (26)$$

One can readily verify that the condition in equation (16) is satisfied for all  $m \geq 1$ , and from equation (17), we find

$$v_R = \beta V_\phi f_m \left( \frac{f_m}{4m^2 - 1} \sin 2m\phi - \frac{2}{m + 1} \sin m\phi \right). \quad (27)$$

It is not difficult to show that  $A(\phi)$  is positive for our simple disks when  $0 \leq |f_m| < 1$ . These disks are analogous to the multiple-lobed disks of G01, but they are not the same. The difference can be traced back to the logic of solving the hydrodynamic equations. In fact, the hydrodynamic equations for self-gravitating disks are four equations for five unknowns,  $\Sigma$ ,  $U$ ,  $v_R$ ,  $v_\phi$ , and  $p$ . Thus, we are free to specify one of these variables or put an extra constraint on them. G01 follow the latter approach and assume an equation of state in the form  $p = a^2 \Sigma$ , where  $a$  is the constant sound speed. They numerically solve their problem for  $\Sigma$ ,  $v_\phi$ , and  $v_R$  and obtain  $U$  through Poisson's equation. Our disks,

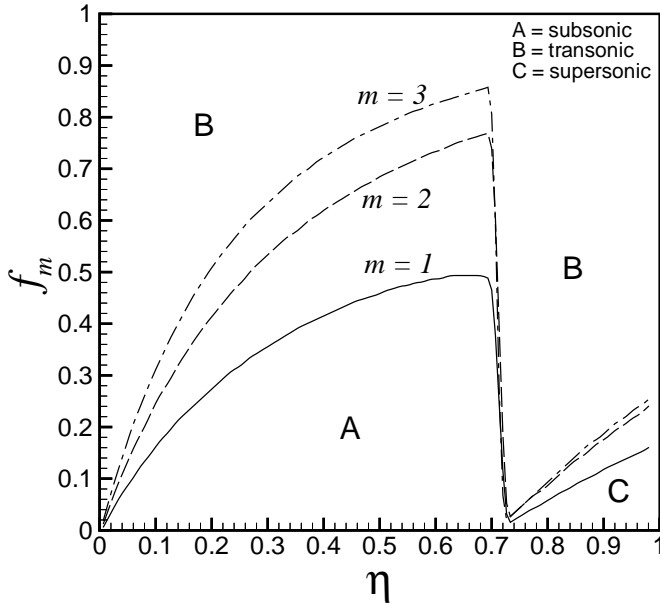


FIG. 1.—Plot of  $(\eta, f_m)$  parameter space of simple disks. The solid, dashed, and dot-dashed lines show the boundary of transonic models for  $m = 1, 2,$  and  $3,$  respectively. More elongated subsonic models are supported as the wavenumber  $m$  is increased. Entirely supersonic models can exist for a limited range of parameters. Such models are almost axisymmetric.

however, are constructed relying on another approach. We prescribe the surface density  $\Sigma$  and find  $U$  using Poisson's integral. Then, we determine  $v_R, v_\phi,$  and  $p$ . Our disks, in contrast to G01, are not isothermal (because the sound speed is not constant according to eq. [19]). Nonetheless, our solutions are exact, and we never face the convergence problem as in G01.

In Figure 1 we have surveyed the  $(\eta, f_m)$  parameter space of our simple disks for  $\pi G = 1, \Sigma_0 = 1,$  and several choices of the wavenumber  $m$ . For each  $m$ , we obtain a curve (solid, dashed, and dot-dashed lines) that is the boundary of models with transonic flow fields. The region to the up side of each curve (indicated by the letter B) corresponds to the models that are transonic along a typical streamline. Below the boundary curve, we obtain entirely subsonic and entirely supersonic regions. Excluding transonic solutions (they are unphysical due to the arguments in § 3.2), highly non-axisymmetric disks can be constructed in the subsonic region as the wavenumber  $m$  is increased. The maximum elongation of the lopsided mode ( $m = 1$ ) occurs for  $f_m \approx 0.5$  and  $\eta \approx 1/\sqrt{2}$ . Whatever the value of  $m$  may be, the maximum value of  $\eta$  is  $1/\sqrt{2}$  for entirely subsonic models. Entirely supersonic models are approximately circular, with  $f_m \lesssim 0.2$ .

#### 4.2. Bisymmetric Disks

There are two interesting families of bisymmetric disks for which self-consistent stellar dynamical models are known. They are the power-law and elliptic disks (JZ02). Disks whose equipotentials are similar concentric ellipses are called “power-law disks.” They are planar analogs of the logarithmic ellipsoidal models (e.g., Binney 1981; Evans, Carollo, & de Zeeuw 2000). The power-law disks with flat rotation curves take the potential of the form in equation

(5), with

$$q(\phi) = \ln(q^2 \cos^2 \phi + \sin^2 \phi), \quad (28)$$

where  $q$  is the axial ratio of equipotentials. The angular dependence of the surface density corresponding to equation (28) has been derived in JZ02 as the following convergent series:

$$f(\phi) = 1 + \sum_{\text{even } l > 0} f_l \cos l\phi, \\ f_l = \sum_{n=1}^{\infty} \left[ \frac{(1-q)^n \delta_{kl}}{2^{n-1}} + \sum_{m=0}^{n-1} \frac{(1-q)^n \beta_m^{(n)}}{2n} (i\delta_{il} + j\delta_{jl}) \right], \quad (29)$$

with  $k = 2n, i = n + m,$  and  $j = n - m$ . In this relation,  $\delta_{rs}$  is the Kronecker delta, and we have defined  $\beta_m^{(n)} = 0$  if  $n - m$  is odd, and

$$\beta_m^{(n)} = \begin{cases} \frac{1}{2^{n-1}} \binom{n}{(n-m)/2}, & m \neq 0, \\ \frac{1}{2^n} \binom{n}{n/2}, & m = 0, \end{cases} \quad (30)$$

if  $n - m$  is even.

When the isodensity contours are similar concentric ellipses, we attain elliptic disks with

$$f(\phi) = (q^2 \cos^2 \phi + \sin^2 \phi)^{-1/2}, \quad (31)$$

where  $q$  is the axis ratio of isodensity contours. Stellar elliptic disks were constructed (for the first time) in K93 and then were examined for self-consistency by the curvature condition in JZ02. The potential function associated with equation (31) was determined by Evans & de Zeeuw (1992, eq. [5.2]) in terms of an indefinite integral, but a practical way is to generate it using the scheme presented in § 3.1. We find

$$U(R, \phi) = 2\pi G \Sigma_0 \left( \ln R - \sum_{\text{even } l > 0} \frac{f_l}{l} \cos l\phi \right), \\ f_l = \sum_{n=1}^{\infty} \sum_{k=0}^n \sum_{m=0}^n (1-q)^n \Gamma \left( \frac{1}{2} + k \right) \Gamma \left( \frac{1}{2} + n - k \right) \\ \times \beta_m^{(n)} (\delta_{il} + \delta_{jl}) [2\pi k! (n-k)!]^{-1}, \quad (32)$$

with  $i = 2k - n + m$  and  $j = 2k - n - m$ . All the series introduced so far rapidly converge using only the first few terms.

For instance, we have computed the isodensity contours and streamlines of our bisymmetric disks for  $q = 0.5, \pi G = 1,$  and  $\Sigma_0 = 1,$  which results in  $A_{\min} = 0.854$  and  $3.041$  for the power-law and elliptic disks, respectively. Figure 2 shows the results of our calculations for several choices of  $V_\phi$ . Solid lines show the isodensity contours, and dashed lines show the streamlines. For small values of  $V_\phi$ , the pressure increases and dominates the centrifugal forces. Therefore, streamlines become highly dimpled in both disks (Figs. 2a and 2c). As the value of  $V_\phi$  is increased ( $V_\phi^2 \rightarrow U_0 A_{\min}$ , i.e.,  $\beta \rightarrow 1/A_{\min}$ ), centrifugal forces overwhelm the pressure forces and keep the fluid particles away from the center. This causes the streamlines to become

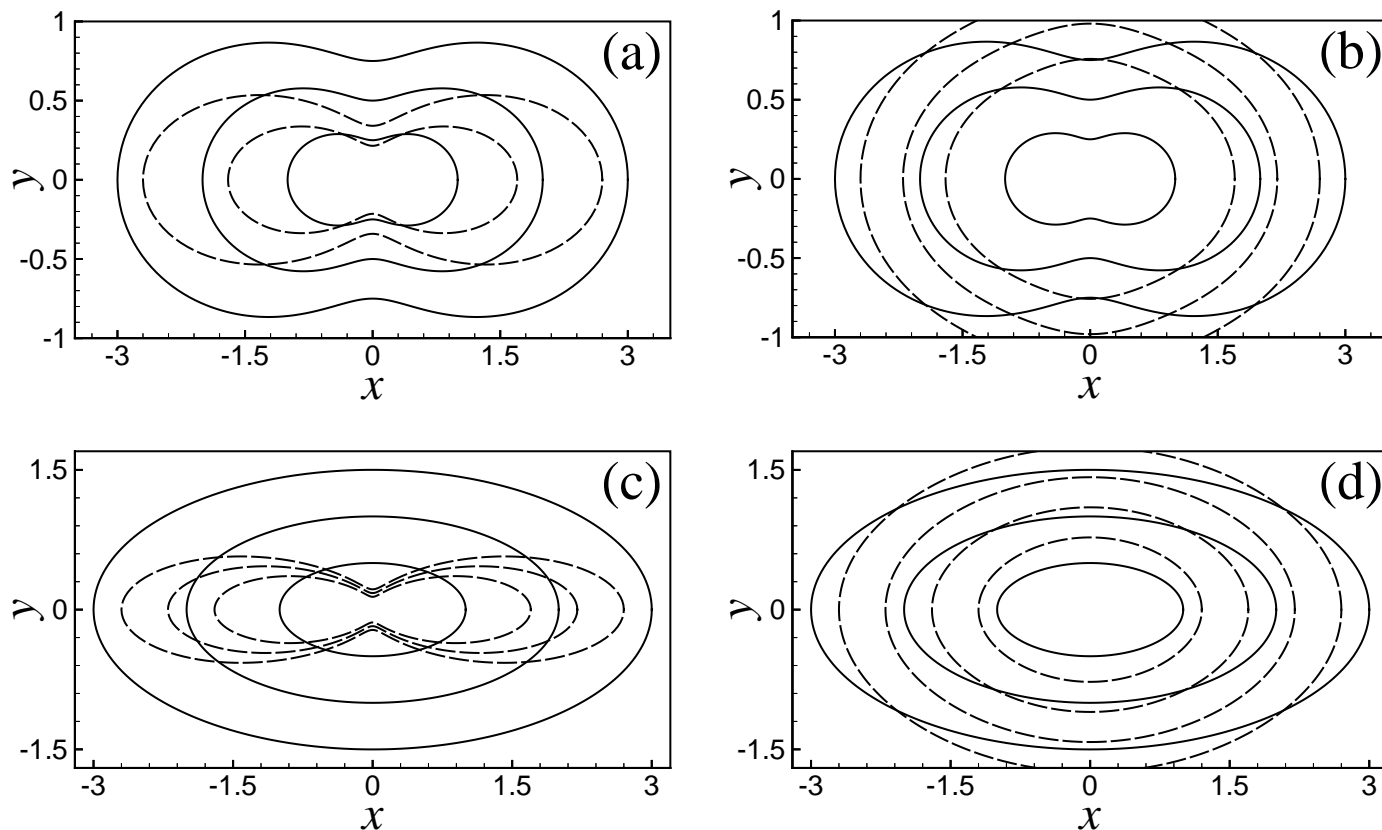


FIG. 2.—Isodensity contours (solid lines) and streamlines (dashed lines) of the power-law and elliptic disks with flat rotation curves for  $\Sigma_0 = 1$ ,  $\pi G = 1$ , and  $q = 0.5$ . (a) Power-law disk with  $V_\phi = A_{\min}^{1/2}/2 = 0.462$ . (b) Power-law disk with  $V_\phi = 4A_{\min}^{1/2}/5 = 0.739$ . (c) Elliptic disk with  $V_\phi = A_{\min}^{1/2}/3 = 0.581$ . (d) Elliptic disk with  $V_\phi = 4A_{\min}^{1/2}/5 = 1.395$ .

rounder (Figs. 2b and 2d). Numerical computations show that  $A(\phi)$  ( $0 \leq \phi \leq 2\pi$ ) is positive for the power-law and elliptic disks in the range  $0 \leq q \leq 1$ . Therefore, it is always possible to find a physical value for  $V_\phi$ . Figure 3 shows the

$(\eta, q)$  parameter space of the power-law and elliptic disks. The shaded region corresponds to models with transonic flow fields. They are most likely unphysical models, as we discussed in § 3.2. Hence, we exclude them from our solu-

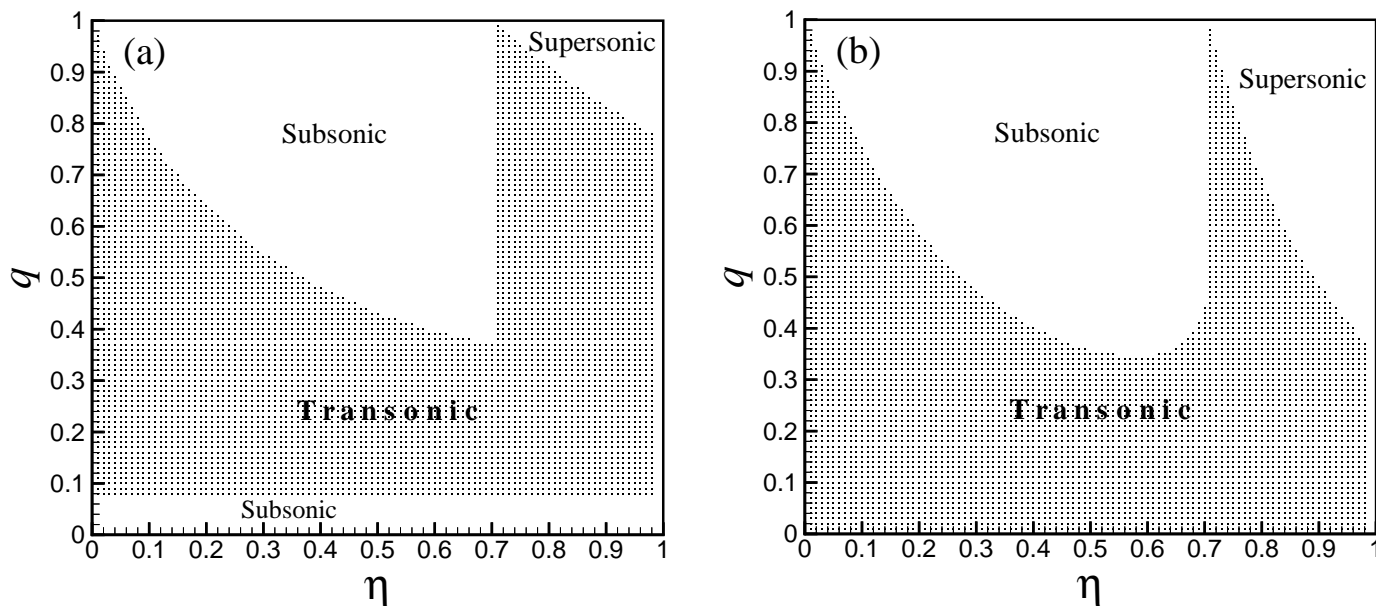


FIG. 3.—Plot of  $(\eta, q)$  parameter space of the (a) power-law and (b) elliptic disks. The shaded region corresponds to models with transonic flow fields, which are most likely unphysical. Elliptic disks allow for more elongated supersonic models than the power-law disks. The maximum value of  $\eta$  taken by subsonic models is equal to  $1/\sqrt{2}$  in both disks.

tion space. As Figure 3 shows, supersonic elliptic disks can be more elongated than supersonic power-law disks. In both cases, the maximum value of  $\eta$  for subsonic flows is equal to  $1/\sqrt{2}$ . This is a generic property of our self-gravitating gaseous disks inherited from simple disks.

Another remarkable point is the limit of the axis ratio  $q$  for plausible models (transonic models excluded). The lower bound of  $q$  is almost 0.4 in elliptic disks, but in the case of power-law disks, one can see a narrow subsonic region with  $q < 0.08$ . In the limit of  $q \rightarrow 0$ , these highly elongated models converge to a needle. The results for elliptic disks are similar to the findings of JZ02 for stellar disks. In fact, stellar elliptic disks with  $q \lesssim 0.5$  are non-self-consistent. On the evidence of Figure 3a, gaseous power-law disks exhibit significantly different features compared to their stellar counterparts, which cannot be self-consistent if  $q < 0.707$  (JZ02).

Our calculations show that the gas pressure of elliptic disks takes an approximately axisymmetric distribution when  $V_\phi$  is small. As a result, the line-of-sight velocity dispersion  $\sigma = \langle v_{\text{los}}^2 \rangle - \langle v_{\text{los}} \rangle^2$  is inversely proportional to  $f(\phi)$ . This property does not depend on the choice of  $q$ , and it predicts a correlation between the photometric and spectroscopic data of elliptic disks when centrifugal forces are dominated by internal stresses.

## 5. IMPLICATIONS FOR THE KINEMATICS OF THE LMC

In his recent study of the LMC, van der Marel (2001) has shown that the LMC disk is elongated and its isophotal lines are well fitted by ellipses. Since the LMC has an approximately flat rotation curve, our elliptic disks (presented in § 4.2) can be applied to model the LMC disk.

The most recent studies of the kinematics of the gas and discrete tracers (such as carbon stars) of the LMC (Kim et al. 1998; Alves & Nelson 2000) show that the line of the maximum velocity gradient is in the range  $143^\circ < \Theta_{\text{max}} < 183^\circ$ , which differs from the angular position of the line of nodes ( $\Theta = 122.5^\circ$ ) by  $20^\circ < \Theta_{\text{max}} - \Theta < 60^\circ$ . Noting the fact that the intrinsic ellipticity of the LMC disk is  $\epsilon = 0.312$  in outer regions, van der Marel (2001) argues that  $\Delta\Theta = \Theta_{\text{max}} - \Theta \approx 20^\circ$  is possible, but it is difficult to believe that  $\Delta\Theta$  can be as large as  $60^\circ$ . He ascribes the excess of computed misalignment to the center-of-mass and rigid-body motions of the LMC. A more accurate kinematic analysis of the LMC predicts a value of  $\Delta\Theta$  as small as  $7.4^\circ$  (R. P. van der Marel 2002, private communication). To provide a theoretical framework for these observations, we have modeled the outer region of the LMC using our elliptic disks.

We have calculated the position angle of the maximum line-of-sight velocity of our elliptic disks, given the viewing angles  $\Theta = 122.5^\circ$  and  $i = 34.7^\circ$  that were determined by van der Marel & Cioni (2001). Our results are shown in Figure 4. This figure illustrates the variation of  $\Delta\Theta$  versus  $\eta$  for several choices of  $\epsilon = 1 - q$ , including  $\epsilon = 0.312$ , which is the intrinsic ellipticity of the LMC at large radii. A discontinuity occurs in the graph of  $\Delta\Theta$  (let us say at  $\eta = \eta_{\text{cr}}$ ) because of a sudden change in the morphology of the streamlines. For  $\eta < \eta_{\text{cr}}$ , the streamlines are dimpled. The graph for  $\epsilon = 0.312$  (squares) shows that  $\Delta\Theta$  varies between  $0^\circ$  and  $30^\circ$  when the streamlines are not dimpled. Interestingly, this result is in harmony with the predictions of van

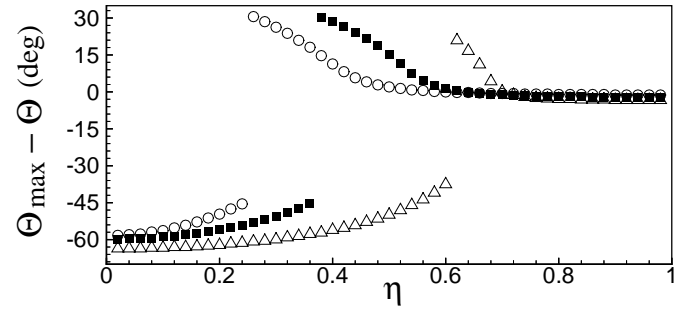


FIG. 4.—Variation of  $\Delta\Theta = \Theta_{\text{max}} - \Theta$  vs.  $\eta = 1/(\beta A_{\text{min}})^{1/2}$  for elliptic disks, given the viewing angles  $\Theta = 122.5^\circ$  and  $i = 34.7^\circ$ . Circles, squares, and triangles correspond to the ellipticities  $\epsilon = 0.15$ ,  $0.312$ , and  $0.6$ , respectively. The existing discontinuities in the data sets are due to a sudden change in the morphology of streamlines. This happens at a critical  $\eta = \eta_{\text{cr}}$ . For  $\eta < \eta_{\text{cr}}$ , the streamlines are dimpled.

der Marel (2001). It is remarked that for  $\epsilon = 0.312$ , we obtain  $\eta_{\text{cr}} = 0.36$ . As  $\eta \rightarrow 1$ , the streamlines become almost circular, independent of the value of  $\epsilon$ . In such a circumstance, the position angle of the maximum line-of-sight velocity coincides with that of the line of nodes, i.e.,  $\Delta\Theta \rightarrow 0$ , as expected. Based on the available observational data and our results for  $\epsilon = 0.312$ , we conclude that our scale-free elliptic disks (with flat rotation curves) can explain the kinematics of the outer region of the LMC if  $\eta$  is chosen in the range  $0.36 < \eta < 0.72$ . The upper bound on  $\eta$  comes from the fact that our transonic solutions are not reliable answers of steady state equations. For  $\Delta\Theta = 7.4^\circ$ , we find  $\eta \approx 0.54$ , which is well within the acceptable range. Moreover, models with  $\eta \rightarrow 1$  (they are supersonic) lead to very high fluctuations of the pressure, and therefore, velocity dispersion. This does not seem to be relevant to a stable model. We also rule out the possibility of  $\eta < \eta_{\text{cr}}$ , for it gives  $\Delta\Theta < 0$ , which is not observed. Furthermore, the condition  $p \rightarrow 0$  at the boundary of the LMC disk is inconsistent with a pressure-dominated model.

## 6. CONCLUSIONS

Exact equilibrium solutions of self-gravitating systems are rare. Two classes of such solutions were found by Medvedev & Narayan (2000) for three-dimensional, axisymmetric isothermal systems. A generalization of these solutions for nonaxisymmetric rotating systems was then introduced by Shadmehri & Ghanbari (2001). Although the density distribution of their models is nonaxisymmetric, the velocity field has only the toroidal component. This makes their models too simple to be used in the study of fully three-dimensional nonaxisymmetric distributions of matter.

In a systematic search for nonaxisymmetric equilibrium solutions, we started our study from gaseous disks because they inherit many properties of three-dimensional systems. Using the benefit of the existence of a stream function, we were successful in reducing the governing equations of scale-free models to an incomplete linear ODE for the angular part of the stream function. It then became clear that Liouville's transformation can reduce the obtained ODE to a second-order inhomogeneous ODE, which is similar to that of a forced harmonic oscillator. This was striking because it led us to derive closed-form solutions for the radial velocity component, stream function, and pressure  $p$ .

In fluid mechanics, transport equations are written for mass, momentum, and energy. While the pressure occurs in governing equations, there is no extra independent equation in order to determine  $p$ . The problem is rather difficult in the presence of an anisotropic stress tensor, which is encountered in turbulence and Jeans' equations of stellar hydrodynamics. Taking the curl of the momentum equations is a trick that temporarily removes the pressure from our calculations of the stream function. However, one should take care of the sign of  $p$  once it is eventually extracted from the momentum equations. Only a positive pressure distribution is physical, because a fluid medium can resist against a compressive stress, but not a tensional one.

Nonaxisymmetric stellar disks have necessarily anisotropic DFs and pressure tensors. This point is the main difference between the physics of a steady state gaseous disk and its stellar counterpart described by Jeans' equations. Nevertheless, isotropic pressure distribution is not an obstacle for the existence of nonaxisymmetric, self-gravitating gaseous disks, as we showed in § 4.

Our scale-free elliptic disks were used to model the outer part of the LMC disk. The main restriction of our

modeling is the isotropy of the stress tensor. We speculate that our results will not be changed in a significant way if the model is stellar with an anisotropic pressure. The other important issue is the perturbation of the Galaxy. The tidal field of the Galaxy induces a force whose  $R$ -distribution is totally different from that of a logarithmic potential field. However, if the tidal field of the Galaxy were dominant, the rotation curve of the LMC would show substantial deviation from flatness. However, we know that the rotation curve of the LMC is almost flat. Therefore, our isolated models provide acceptable *zero-order* solutions. Such a modeling of the LMC is a quick route for interpreting the observational data. It is obvious that taking the tidal effects into account will destroy the enjoyable scale-free nature of our disks.

We thank Tim de Zeeuw for useful comments and for drawing our attention to the possible application of our findings to the LMC. We are indebted to the anonymous referee for enlightening suggestions that helped us to substantially improve the presentation of our results.

## APPENDIX

### LIOUVILLE'S TRANSFORMATION

Consider the following nonautonomous, linear ODE for  $Z$  in terms of  $t$ :

$$\frac{d^2 Z}{dt^2} + Q_1(t) \frac{dZ}{dt} + Q_2(t)Z = Q_0(t). \quad (\text{A1})$$

Using the transformation (Bellman 1966, p. 82; Verhulst 1996, problem [8-2])

$$Z(t) = w(t) \exp \left[ -\frac{1}{2} \int_0^t Q_1(\tau) d\tau \right], \quad (\text{A2})$$

which has been introduced by Liouville, equation (A1) becomes

$$\frac{d^2 w}{dt^2} + \left( Q_2 - \frac{1}{2} \frac{dQ_1}{dt} - \frac{1}{4} Q_1^2 \right) w = Q_0(t) \exp \left[ \frac{1}{2} \int_0^t Q_1(\tau) d\tau \right]. \quad (\text{A3})$$

The study of this equation is easier than equation (A1).

We assume  $P'$  as the dependent variable. This puts equation (11) in the form of equation (A1). We then apply equation (A2) and obtain equations (12) and (13).

## REFERENCES

- Alves, D. R., & Nelson, C. A. 2000, *ApJ*, 542, 789  
 Anderson, J. D. 1990, *Modern Compressible Flow* (New York: McGraw-Hill)  
 Bellman, R. 1966, *Perturbation Techniques in Mathematics, Physics and Engineering* (New York: Dover)  
 Binney, J. 1981, *MNRAS*, 196, 455  
 Binney, J., & Tremaine, S. 1987, *Galactic Dynamics* (Princeton: Princeton Univ. Press)  
 de Zeeuw, P. T., Hunter, C., & Schwarzschild, M. 1987, *ApJ*, 317, 607  
 Evans, N. W., Carollo, C. M., & de Zeeuw, P. T. 2000, *MNRAS*, 318, 1131  
 Evans, N. W., & de Zeeuw, P. T. 1992, *MNRAS*, 257, 152  
 Galli, D., Shu, F. H., Laughlin, G., & Lizano, S. 2001, *ApJ*, 551, 367 (G01)  
 Goodman, J., & Evans, N. W. 1999, *MNRAS*, 309, 599  
 Heemskerk, M. H. M., Papaloizou, J. C., & Savonije, G. J. 1992, *A&A*, 260, 161  
 Jalali, M. A., & de Zeeuw, P. T. 2002, *MNRAS*, 335, 928 (JZ02)  
 Kim, S., Staveley-Smith, L., Dopita, M. A., Freeman, K. C., Sault, R. J., Kesteven, M. J., & McConnell, D. 1998, *ApJ*, 503, 674  
 Kuijken, K. 1993, *ApJ*, 409, 68 (K93)  
 Lemos, J. P. S., Kalnajs, A. J., & Lynden-Bell, D. 1991, *ApJ*, 375, 484  
 Levine, S. E., & Sparke, L. S. 1998, *ApJ*, 503, 125  
 Medvedev, M. V., & Narayan, R. 2000, *ApJ*, 541, 579  
 Mestel, L. 1963, *MNRAS*, 126, 553  
 Schwarzschild, M. 1979, *ApJ*, 232, 236  
 Shadmehri, M., & Ghanbari, J. 2001, *ApJ*, 557, 1028  
 Syer, D., & Tremaine, S. 1996, *MNRAS*, 281, 925 (ST96)  
 Teuben, P. 1987, *MNRAS*, 227, 815  
 van der Marel, R. P. 2001, *AJ*, 122, 1827  
 van der Marel, R. P., & Cioni, M.-R. L. 2001, *AJ*, 122, 1807  
 Verhulst, F. 1996, *Nonlinear Differential Equations and Dynamical Systems* (2d ed.; Berlin: Springer)